ECS Transactions, 19 (29) 55-74 (2009)
10.1149/1.3259799 ©The Electrochemical Society

Electromagnetic Induction Corrosion Control Technology (EICCT)

Digby D. Macdonald[1], Michael Lewis[2], Jason McLafferty[2], and Randy Peek[3]

[1]Center for Electrochemical Science and Technology
Department of Materials Science and engineering
Pennsylvania State University
University Park, PA 16802

Tel: (814) 863-7772; Fax: (814) 863-4718; E-mail: ddm2@psu.edu

[2]Lewis Research & Engineering
13345 Market Ave. N.
Hartville, Ohio 44632
Tel: (330) 354-8101; E-mail: melewis@raex.com

[3]Randy Peek, CEO
Canadian Auto Preservation Inc.
390 Bradwick Drive
Concord, Ontario L4K 2W4
Canada
Tel: (905) 660-9615 Ex. 226; E-mail: randy@capfinalcoat.com

Over the past several years, a new corrosion control technology has been developed for protecting damaged, painted steel surfaces in contact with ambient atmospheres. The method makes use of electromagnetically-induced surface currents and, to date, the efficacy of the method has been demonstrated with painted, galvanized steel. While the exact mechanism of protection has yet to be thoroughly defined, the technique appears to work by the induced current inhibiting passivation of the zinc and hence maintaining the zinc in the active state. Accordingly, the active zinc is more effective in protecting the underlying steel, as a sacrificial anode, compared with passivated zinc in the absence of the electromagnetically-induced current. Thus, the technique is not a classical, impressed current cathodic protection system and no electrolyte is needed between an anode (which does not exist, anyway) and the damaged area. Experiments have demonstrated that the induced current is spread uniformly across the surfaces of complex shapes, such as automobile bodies, so that induction at a single point is effective in protecting the whole body, that the power consumption is very low, and possibly that the induced signal can be tailored to optimize the efficacy. To our knowledge, EICCT is a new, radically different corrosion control technology that may find extensive application in protecting metallic structures.

Introduction

This paper describes the evaluation of a new corrosion control technology, Electromagnetic-Induced Corrosion Protection (EICP)**,** which has been found to effectively protect painted, galvanized steel panels, in which the surface has been damaged to the extent that the damage extends through the coating and the underlying galvanizing to the base steel. To our knowledge, this technology has not been previously described, but its efficacy is such that it might find widespread use in protecting painted, galvanized steel structures (e.g., automobile bodies, light standards, and highway railings). The surface currents that are postulated to be responsible for protection are induced into the metal structure by a pulse generator, hereafter termed the "Module", with the structure essentially operating as an antenna. Some technical details of the Module are given below.

The experiments described below were performed to examine the efficacy of EICCT to protect a damaged surface in the absence of an electrolyte film between the point of damage and the point at which the electrical signal from the Module is applied and, to the extent possible, to indicate the mechanism by which the Module provides protection against corrosion. One of the principal problems in assessing the effectiveness of the Module lies in ascertaining exactly how the device achieves corrosion control, since it is not a classical impressed current cathodic protection system, in which dc current is projected through a ionically conducting (aqueous) phase from an anode to the region that needs to be protected, such that the potential of the region at which steel is exposed to the environment is displaced in the negative direction. The testing described below measures the Module's effect on the potential of a scribed region (exposed steel) on a test panel in the absence of an electrolyte film (aqueous phase) between the point of application of the electrical signal from the Module and the area being protected. Under these circumstances, classical, impressed current cathodic protection is impossible, because a return path for the current from the scribe to the anode through an electrolyte film does not exist and because no anode exists on the surface. Accordingly, a positive result from these experiments will demonstrate that the:

1. Module is effective in protecting painted, galvanized steel panels, as evidenced by a shift in the potential of the exposed steel at the scribe in the negative direction.
2. Mechanism of protection provided by the Module is not that of classical, impressed current cathodic protection.

Additionally, as indicated below, the current or voltage applied to a panel by the Module is in the form of a repetitive pulse and not as a direct current that is employed in impressed current cathodic protection systems, again demonstrating a vital difference between the latter and the Module. Work is currently underway to enhance the efficacy of EICCT by tailoring the form of the induced current delivered by the module.

Experimental

The current paper describes four sets of experiments that were carried out to evaluate the efficacy of EICCT. For each set of experiments, two standard automobile stock galvanized steel panels each measuring 4 feet by 3 feet were coated on both sides with DUPONT WA5111 coating and then clear-coated on one side only with DUPONT 72400 by Northwest Campus Auto Body located in Columbus, Ohio. This is a standard coating system for exterior automobile bodies. The panels were identical in all material respects.

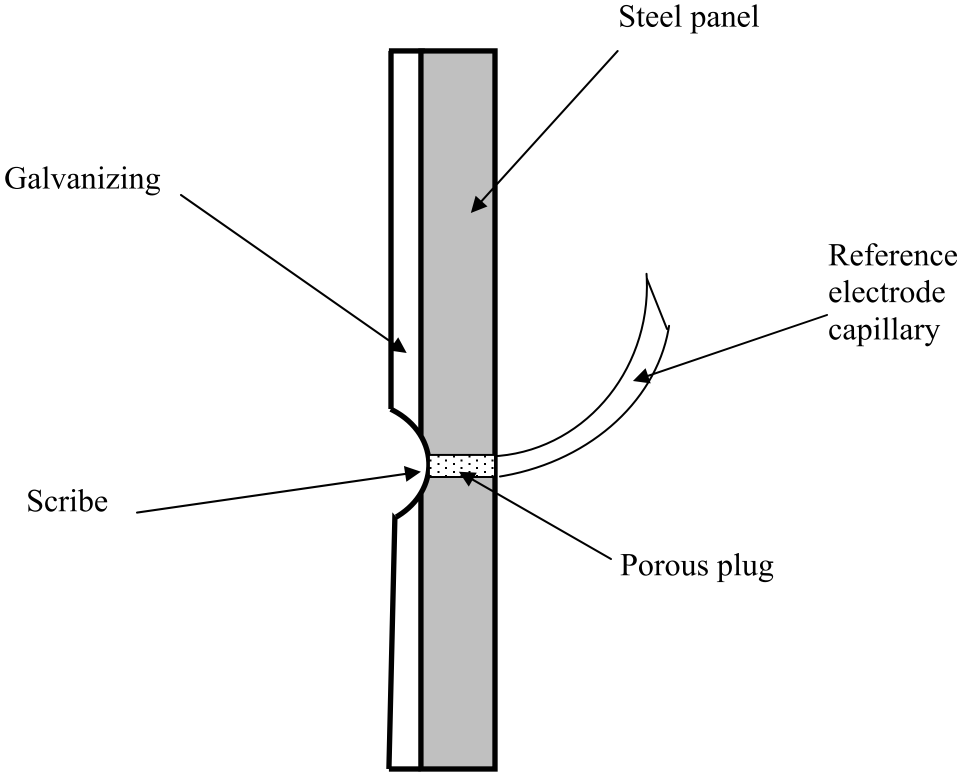

Figure 1: Schematic of the reference electrode connection, showing the Luggin probe (reference electrode capillary) on the back-side of the panel and the liquid junction (“porous plug”) protruding through a 1/16” hole drilled through the panel at the scribe.

The panels were scribed to cut through the clear coat, paint, and galvanized layer, thereby exposing the bare steel. A reference electrode was placed at the location of the scribe on each panel to monitor the corrosion potential of each panel. The reference electrode comprised a Ag/AgCl + KCl(sat) active element and employed a Luggin capillary connected to the panel from the back side (Figure 1). Electrolytic communication between the scribe and the liquid junction of the Luggin capillary was affected by a small diameter (1/16-inch) hole through the panel. The potential of the exposed steel at the scribe, as measured against the reference electrode, was recorded using a high impedance voltmeter/data logger.

The reference electrode shown schematically in Figure 1 was mounted upon both a test panel (equipped with a Module) and a control panel (no Module) exposed to the environment under identical conditions. In the case of the Test Panel, the Module was placed on the back side of the panel with the lead wire also being attached at the same general location (rear of the panel). In this way, any possibility of the inadvertent development of an electrolyte path between the module connection to the panel and the scribe was eliminated. The connection of the Module to the backside of the Panel and the entire electrical circuitry is shown in Figure 2.

Both panels were inclined at approximately 25 degrees to the vertical with the scribed surface facing outward and with the scribe being located approximately 3 feet down from the top edge. The scribed surfaces of the panels were continuously sprayed with a 3.6 wt.% NaCl (salt) solution to simulate road salt exposure. Only the surface of the panel in the vicinity of the scribe was inundated with the electrolyte (see Figure 3); the remainder of the panel surface was dry. In fact, the distance between the top of the spray zone and the location where the Module was connected to the Test Panel was approximately 2 feet. In addition, as noted above, the lead wire for the Module was connected to the back of the Test Panel, which was not in contact with the electrolyte plume.

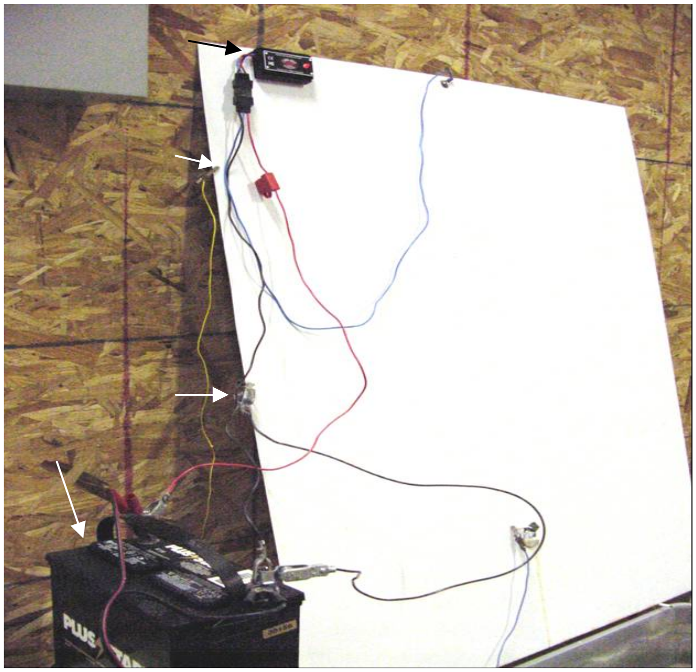

Figure 2: View of Module connection (black arrow) at back of the panel, also showing the ground connection and battery power supply.

With the exception of the presence of the Module on the Test Panel, the configuration of the Test Panel and Control Panel was identical in all material respects. The configuration of the Test Panel is described in the schematic diagram found at Figure 3 below. The actual test arrangement is also shown in the photographs found at Figures 4 and 5 below. The progression of corrosion was quantified by measuring the corrosion potentials and was also characterized visually by examining the rust stains emanating from the scribes.

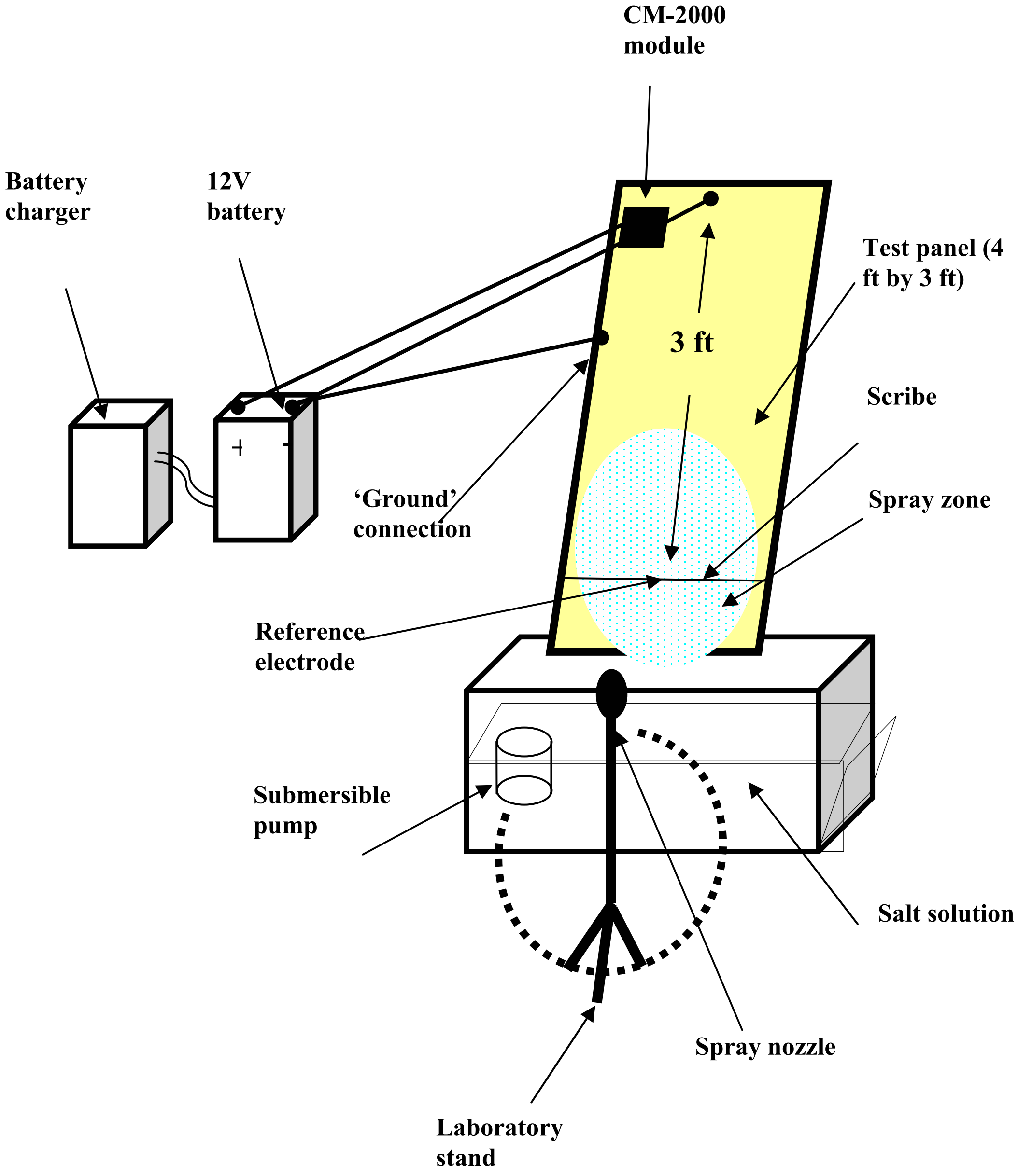

Figure 3. Schematic of the test apparatus showing the location of the panel, the spray nozzle, and the control module.

Results and Discussion

As outlined in greater detail below, the Test Panel (which was connected to the Module) showed marked differences in corrosion potentials when compared with the

Control Panel. The experiment was conducted on four occasions using four different sets of panels. In each case, the panels were prepared and tested in accordance with the methodology described above. Each of the four runs of the experiments yielded broadly consistent results. Specifically, the potential for the Test Panel eventually became more negative than that for the Control Panel by approximately 150 mV. In addition, the difference in corrosion potential was also supported by the difference in the rust staining characteristics of the Test Panel when compared with the Control Panel.

Figure 4: View of test system from above the nozzle stand. The scribe in the panel is shown as the rust line across the width of the panel.

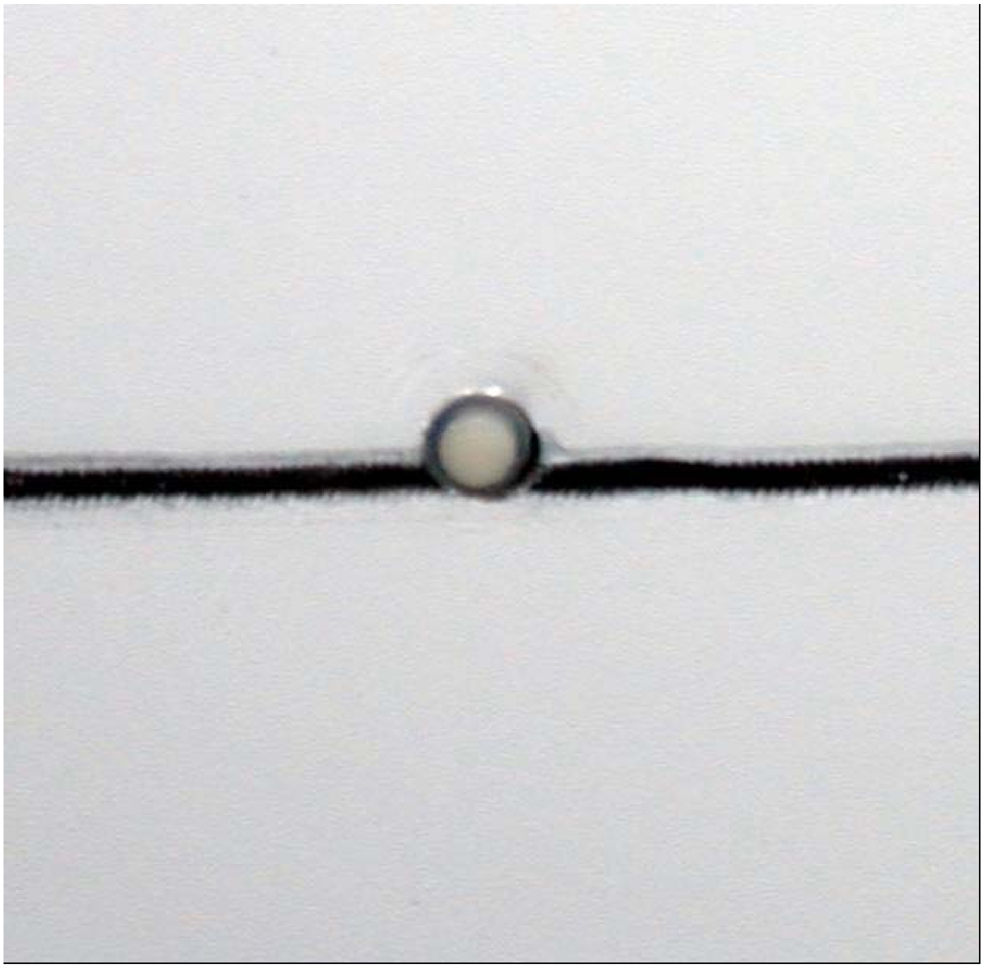

Figure 5: Close-up of the tip of the reference electrode Luggin probe extending through a 1/16” hole from the back of the scribe.

During the first run of the experiment, the corrosion potentials measured at the scribes on both panels were approximately the same until the test had been conducted for approximately 60 hours. The potentials then diverged, with that for the Test Panel eventually becoming more negative than that for the Control Panel by approximately 150 mV. This significant difference in corrosion potential continued until the experiment was terminated following 550 hours of exposure. A chart showing the corrosion potential versus time over the duration of the entire experiment for the Test Panel and Control Panel is given in Figure 6. In this figure, it is seen that, initially, the potential from both panels drifted in unison in the positive direction, which is consistent with passivation of the zinc. However, after about 60 hours of exposure, the potentials of the two panels diverged with that of the panel controlled by the Module becoming more negative by about 150 mV. It is also noted that the "noise" in the Test Panel potential is significantly greater than that for the Control Panel. The fluctuations in the Test Panel potential are to be expected, because the panel is under active electrochemical control from the Module, in which the efficacy of the Module may vary from time-to-time as the local conditions change (e.g., the growth and detachment of gas bubbles). In any event, the efficacy of the Module in displacing the potential of the scribed area in the negative direction is clear.

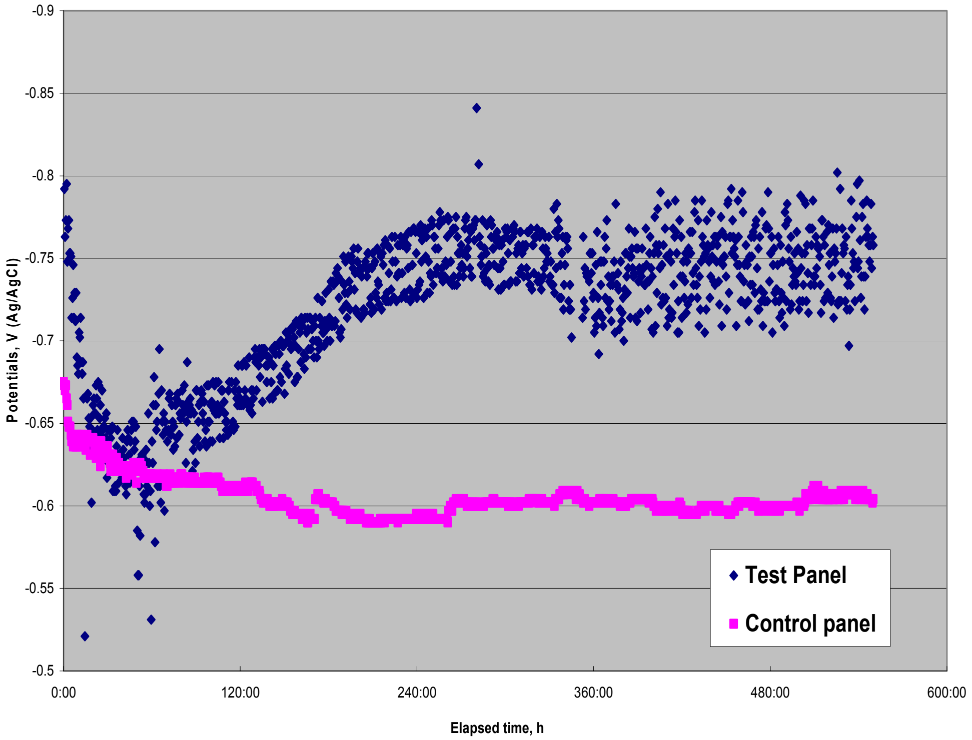

Figure 6: Potential versus elapsed time curve for Experiment No. 1. Note that the potentials of both the test (with the Module) and the control (no Module) panels initially move in unison to more positive values, but that after about 100 hours the potential diverge with that for the test panel moving to more negative values, consistent with reactivation of the zinc galvanizing. Note, further, that the induction time (time over which the potentials of the two panels are coincident) is about 50 hours.

The difference in corrosion potential is also supported by the difference in the rust staining characteristics of the Test Panel, when compared with the Control Panel. Photographs of the two sets of panels are shown in Figures 7 and 8, respectively. These tests showed marked differences in the extent of rust staining from the scribes on the Test Panel and the Control Panel from very short times.

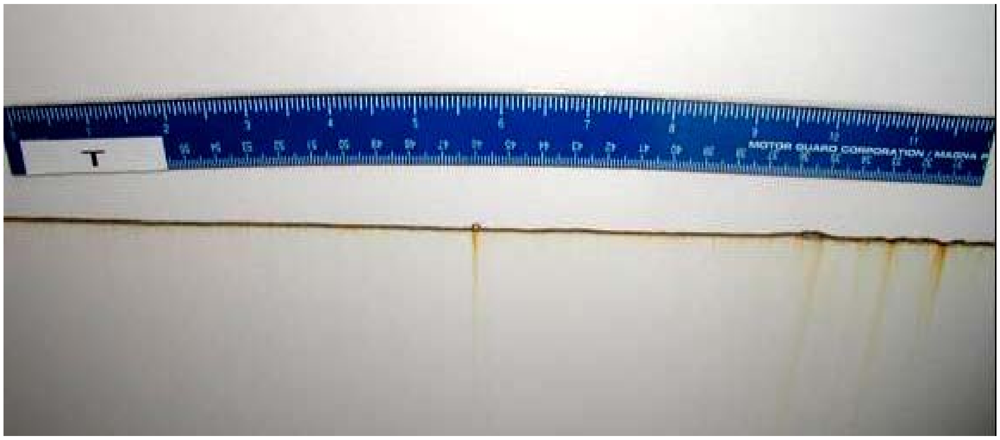

Figure 7: Test panel appearance after 550 hours of exposure (Experiment No. 1). Note the small amount of rust emanating from the scribe, compared with that for the control panel (Figure 8).

The fact that *any* staining is observed on the Test Panel can be attributed to the fact that an induction period exists for the efficacy of the Module to develop. Thus, with reference to Figure 6, the impact of the Module on the corrosion potential of the scribe is evident only after about 100 hours of exposure, during which time rust would have accumulated on the Test Panel to the same extent that it accumulated on the Control Panel. In other words, we postulate that the rust that accumulates on the Test Panel did so during the induction period. After that time, very little corrosion, if any, occurs as the Module takes effect. Because, in automobile protection, we are concerned with long term effects (>> 100 hours), we conclude that the module is effective to the extent that little or no additional rust staining would have been observed after the initial 100-hour exposure period. Clearly, any staining that would have occurred during the induction period might reasonably be expected to be cleaned from the automobile body early in the life of the vehicle. The present data suggest that, thereafter, the accumulation of rust staining on a vehicle protected by the Module should be minimal, if not non-existent.

As noted above, the experiment was repeated on four separate occasions, with broadly consistent results. The time required to establish a significant difference in corrosion potential was longer and visual evidence of rust staining was more or less than in the first run of the program. This is consistent with the existence of an induction time for the Module to begin to exert control over the corrosion process, as noted above, and it is the goal of future work to understand the processes that control the length of the induction period. However because long-term protection is the goal of automobile corrosion mitigation, the initiation period is of no practical significance. The results of the second, third, fourth, and fifth rounds of the testing are shown in Figures 9 to 16 below.

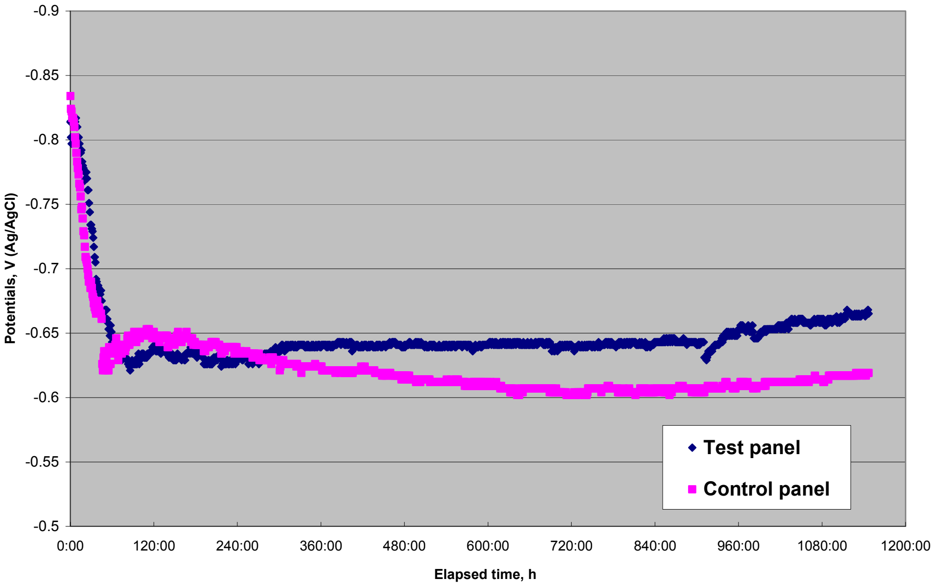

Figure 9: Potential versus elapsed time curve (Experiment No. 2). Note that, in this case, the maximum difference in the potentials of the test and control panels was only 50 mV compared with 150 mV for Experiment No. 1. In spite of this small potential difference, a clear difference exists in the rust staining characteristics of the panels (Figures 10 and 11). Note, further, that the induction time is approximately 250 hours.

Figure 10: Test panel appearance (Experiment No. 2)

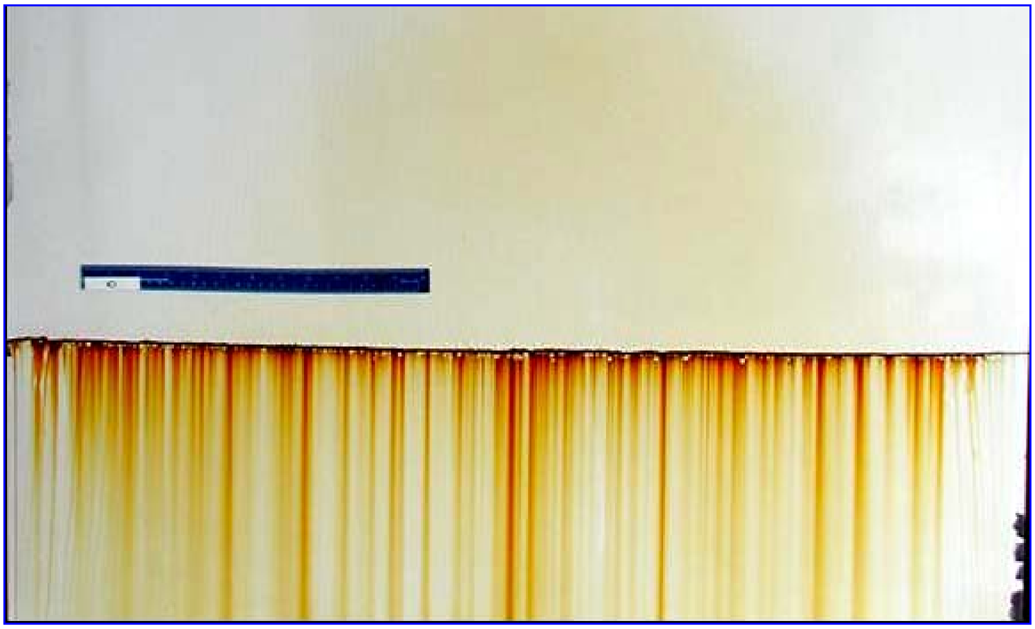

Figure 11: Control panel appearance (Experiment No. 2).

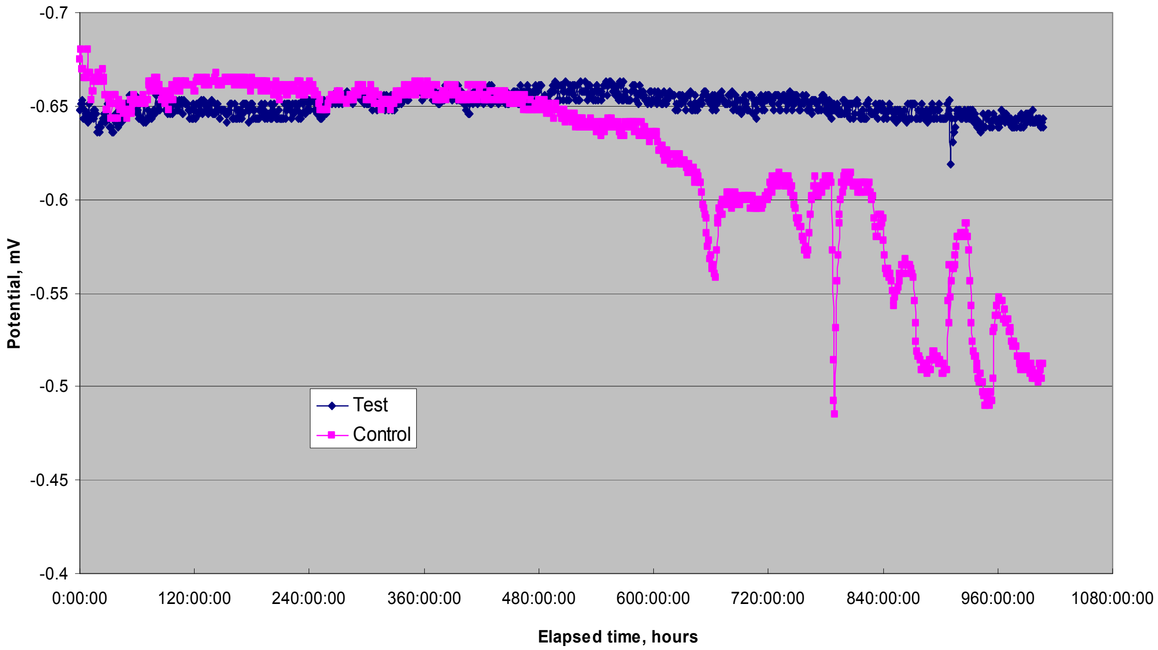

Figure 12: Potential versus elapsed time curve (Experiment No. 3). In this case, the potentials of the two panels were coincident for the first 500 hours and then diverged with the potential of the control panel drifting in the positive direction. The relatively small difference observed in the rust staining characteristics of the panels (Figure 13 and 14) can be attributed to the long induction period over which no difference exists in their corrosion characteristics.

Figure 13: Test panel appearance (Experiment No.3).

Figure 14: Control panel appearance (Experiment No. 3).

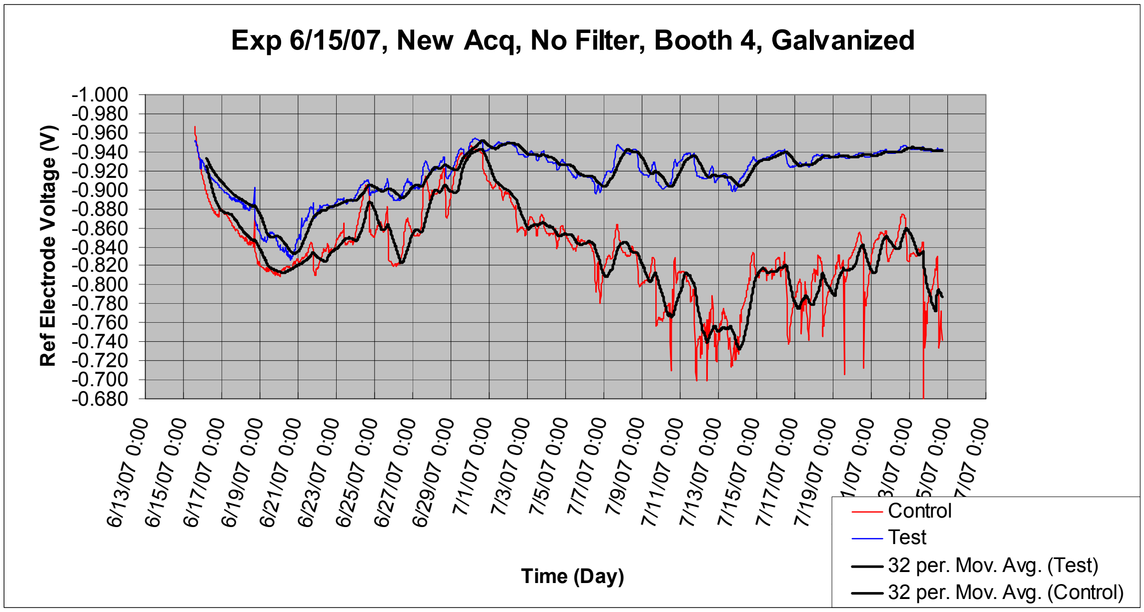

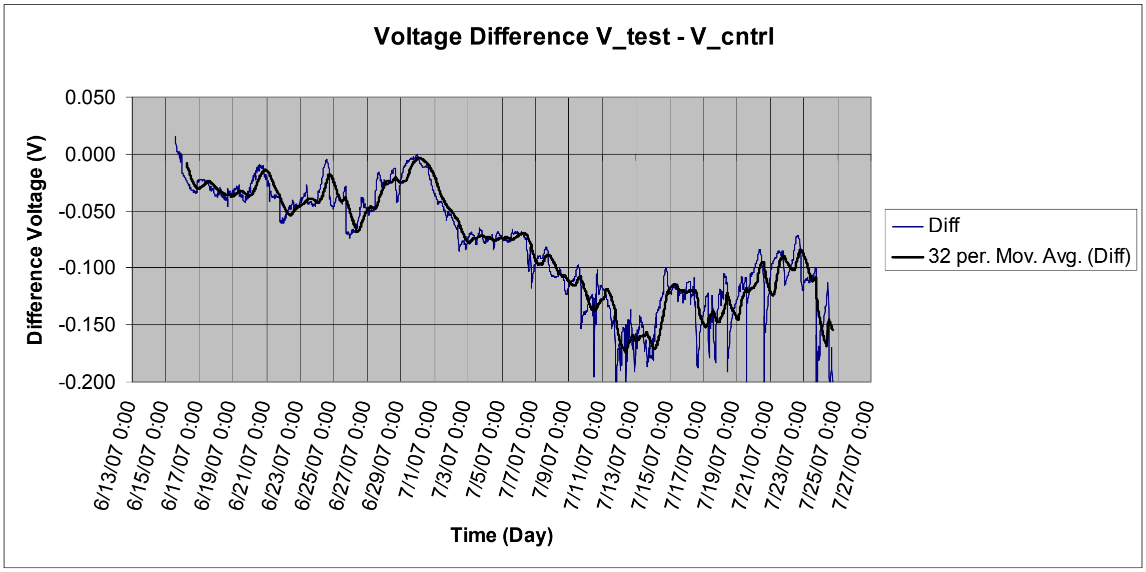

Figure 15: Potential of the test and control panels and potential difference versus time for Experiment No. 4.

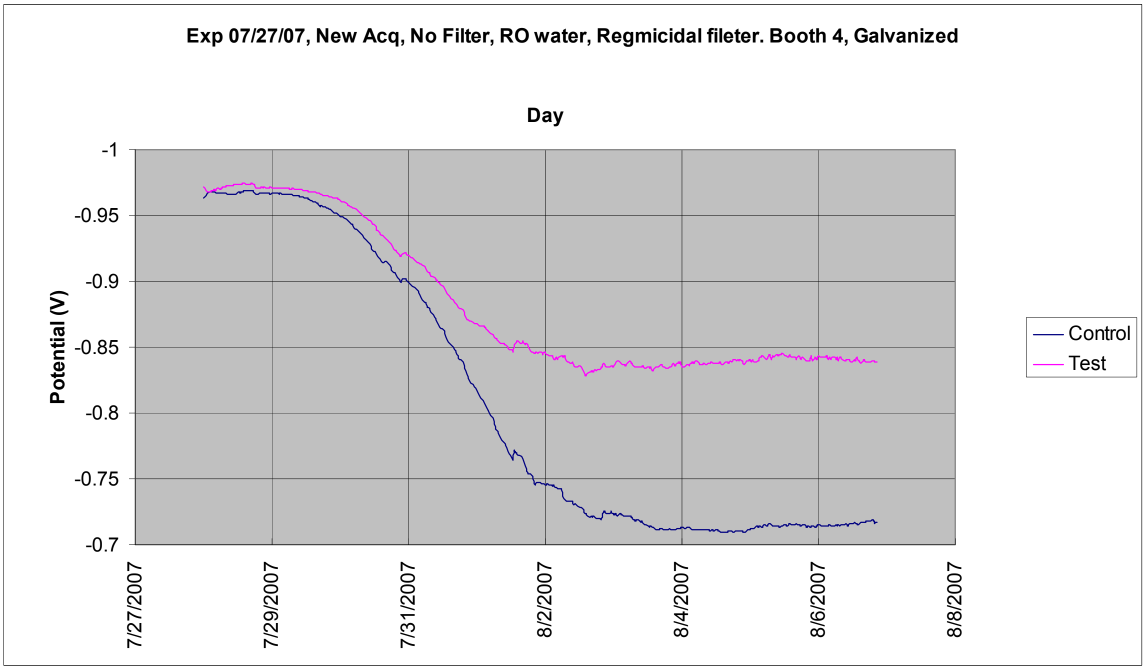

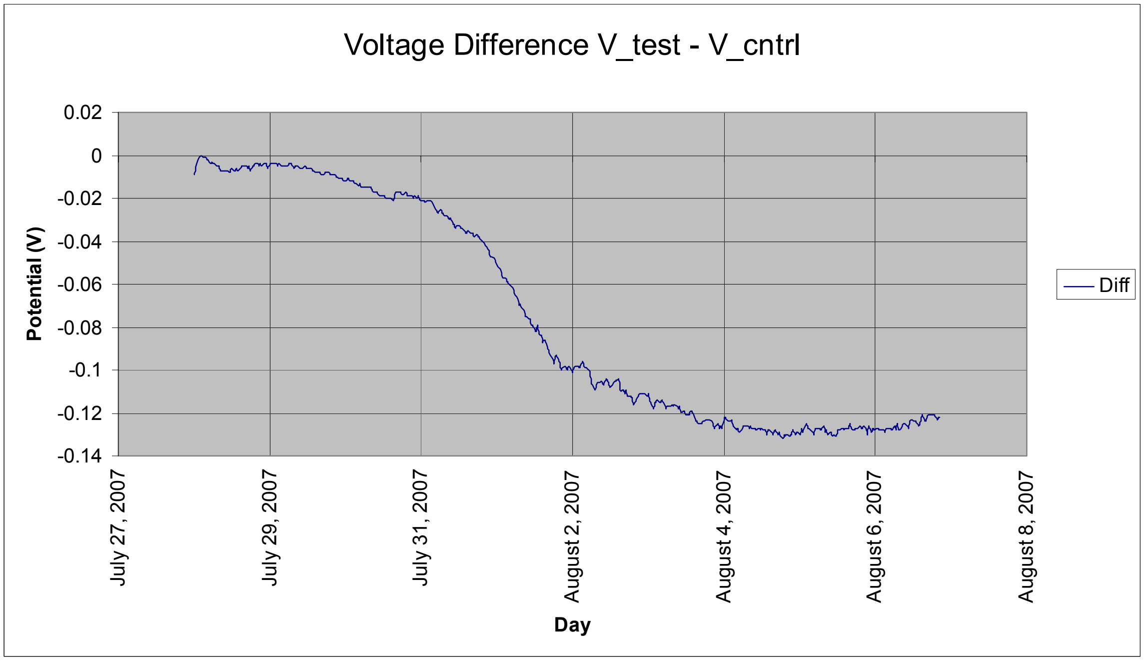

Figure 16: Potential of the test and control panels and potential difference versus time for Experiment No. 5.

The effect of a 150mV difference in the corrosion potential on the rate of corrosion of an automobile body panel is significant and may be determined by applying the following formula, which is derived from electrochemical kinetic (Tafel) theory:

$$CR = (CR)_0 exp\ (\alpha F E_{corr}/RT) \qquad [1]$$

where CR is the corrosion rate, $(CR)_0$ is a constant, α is the transfer coefficient, F is Faraday's constant (96,487 C/equiv.), R is the universal gas constant (8.314 J/K.mol), T is the Kelvin temperature (298.15 K), and E_{corr} is the corrosion potential. This equation holds for all values of the corrosion potential and hence we may write:

$$(CR)_{test}/(CR)_{control} = exp\{\alpha F[E_{corr/test}-E_{corr/,control}]/RT\} \qquad [2]$$

where $E_{corr/test}-E_{corr/,control} = -0.150$ V and $\alpha = 1.0$ (1). Substitution of the values for the various parameters (1) yields $(CR)_{test}/(CR)_{control} = 0.00291$. That is, the corrosion rate is reduced by 99.7 % by the Module on the Test Panel compared with the Control Panel Even if the difference in the corrosion potential is reduced to –0.100V, the ratio $(CR)_{test}/(CR)_{control} = 0.0204$ and hence the corrosion rate is reduced by 98 %. To put these numbers in perspective, imagine that a system (automobile) fails by corrosion without the Module in a time of one year. If the Module were attached, the failure time would be 343 years, if the potential is displaced by 150mV in the negative direction and 49 years if the potential was displaced by only 100mV. Such results are particularly significant when one considers that the average life of a vehicle is of the order of 10 years. Accordingly, these calculations demonstrate that the reduction in corrosion rate is substantial and that the Module is an effective corrosion control device.

Careful consideration of the results obtained to date leads us to postulate that the Module reduces the rate of corrosion by limiting the passivation of the zinc galvanizing, thereby enhancing the efficacy of galvanization in protecting the underlying steel. As evidenced by the experiment described herein, the Module does not require a continuous aqueous phase to exist between the corrosion site and the point of application of the electrical signal. The Module utilizes a high frequency AC induced current that operates on the surface similar to an antenna. The current profile for the Module is presented in Figure 17: The reader will note that the current pulse has a rise time of about 100 μs and a duration of approximately 3.5 μs. Using the time to frequency conversion theorem, the frequency content of the applied signal is 0.01 MHz to 3.5 MHz. At this higher frequency, the induced current is concentrated near the surface,; i.e., it is concentrated in the region at which corrosion occurs.

The data for the above current profile was recorded using an HP 54100D Digitizing Oscilloscope. The current shown is the current in the blue wire of the Module that is connected to the Test Panel. From the plots provided it is clear that the current pulse is not a DC type but is a pulsed AC type, and hence that the technique does not meet the conditions demanded by impressed current cathodic protection.

As one can see, the current rises predominantly in the positive direction at the leading edge of the voltage pulse, followed by a pulse of current predominantly in the negative direction. This is to be expected, since the current in the blue wire is passed through a capacitor and is related to the time derivative of the voltage across the capacitor, as given by:

$$I = C\frac{dV}{dt} \qquad [3]$$

where I is the current through the capacitor and hence through the blue wire (the capacitor is connected to the blue wire), C is the capacitance, V is the voltage pulse across the capacitor (shown in a graph in the presentation), and t is time. At the leading edge of the voltage pulse, the time derivative dV/dt is strongly positive resulting in a positive current, while at the trailing edge of the pulse the time derivative is strongly negative resulting in a negative current. Neither current pulse is entirely positive or negative, because neither the leading edge nor the trailing edge of the voltage pulse V monotonically increases or decreases. This is due to the fact that there are ripples on both the leading edge and trailing edge caused by ringing of the voltage waveform, which itself is due to resonances caused by parasitic inductances, such as those due to the wires themselves. Also, the time between the current pulses is 4.26 μS. This is in keeping with the nominal pulse width of the rust inhibitor unit of 4.0 μS

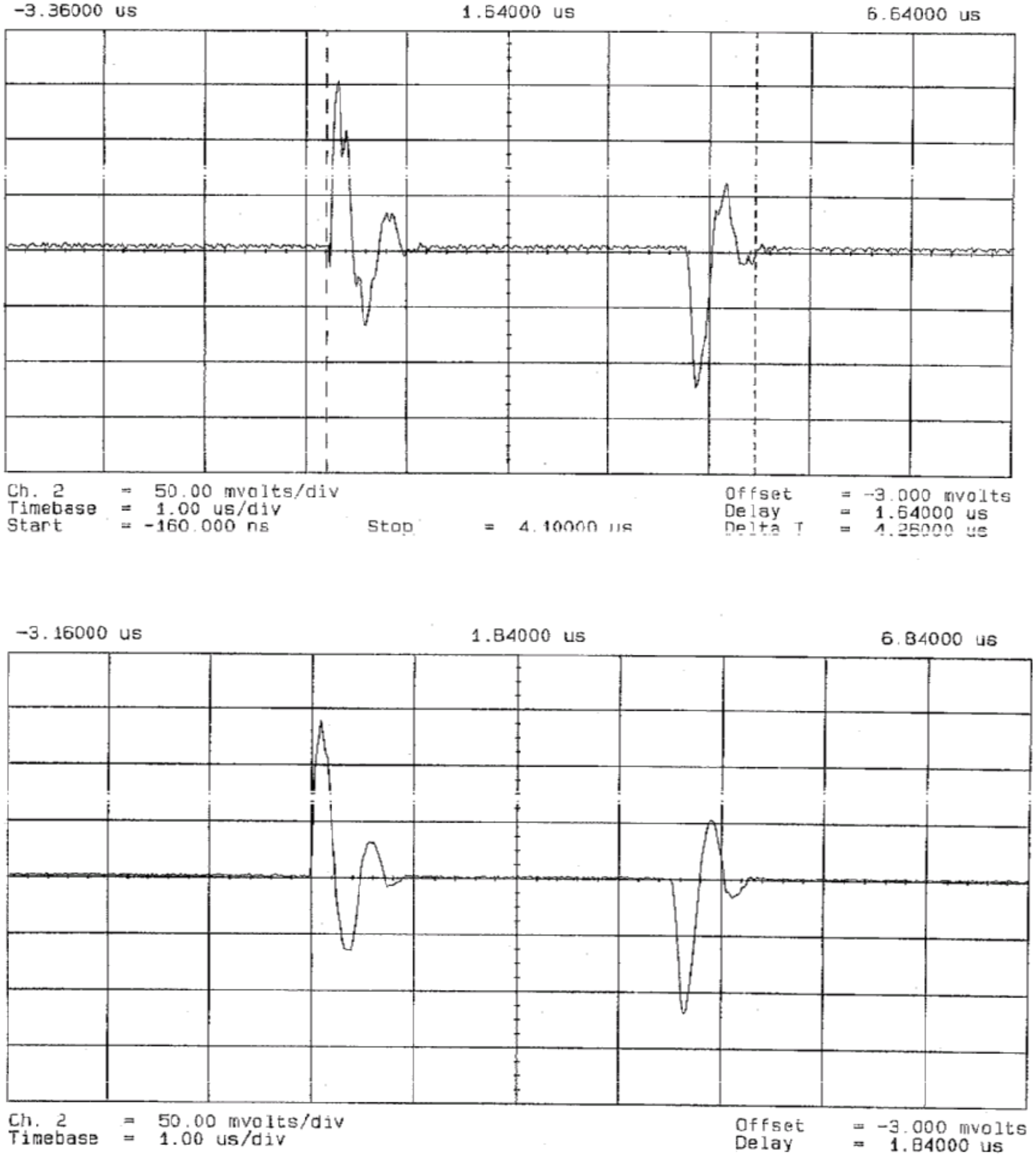

Figure 17: Current profile for the Module.

Unlike impressed current cathodic systems, the Module's effect is not limited to the region where a continuous electrolyte film exists between the point of application of the electrical signal (the anode) and the area being protected. Rather, similar to an antenna, the current from the Module covers the entire surface and does so instantly (at the speed of light, a result that is predicted by Maxwell's equations). As such, the Module is effective in reducing the rate of corrosion over the entire surface of a vehicle. This latter aspect was explored by the Electrosciences Laboratory at Ohio State University, using an actual automobile (a Buick Century) as the test specimen (2). The induced current was detected using a "wand" coil as the detector at fifty-eight locations across the body of a Buick Century automobile and it was found that the induced current was uniformly distributed across the entire surface in spite of the complex shape of the automobile. This result is fully consistent with modern electrodynamics.

It is evident from the potential versus time data plotted in Figures 6, 9, 12, 15, and 16 that a considerable induction time may exist before the Module causes reactivation of the galvanizing. For these five experiments, the induction times were 50 hours, 250 hours, 450 hours, 384 hours, and 72 hours, respectively. Indeed, two experiments were conducted in which the systems remained within the induction period for approximately 1000 hours, and hence little difference was observed in the rust staining characteristics (see, for example, Figures 12, 13, and 14). Note that Figure 12 shows that little difference exists between the panels over half of the experimental time and that upon termination of the experiment, the difference amounted to no more than 0.1 V. As emphasized earlier, we currently do not know in mechanistic detail what determines the length of the induction period, but it is presumably related to the kinetics of breakdown of the passivated zinc surface adjacent to the exposed underlying steel. The defective oxide barrier layer on passive zinc, $Zn_{1+x}O_{1-y}$ is an n-type semiconductor by virtue of the excess of cation interstitials and oxygen vacancies as the principal point defects (3, 4). It is believed that the majority of the passive current is carried by the cation interstitials, which are generated at the metal/barrier layer (m/bl) interface by $Zn \rightarrow Zn_i^{2\bullet} + v_{Zn} + 2e^-$ and are annihilated at the barrier layer/solution (bl/s) interface by the reaction $Zn_i^{2\bullet} \rightarrow Zn_s^{2+}$, where $Zn_i^{2\bullet}$, v_{Zn}, and Zn_s^{2+} are the zinc interstitial, the zinc vacancy on the metal side of the m/bl interface, and the zinc cation in the aqueous solution, respectively. If the electromagnetically-induced current being driven though the barrier layer is sufficiently high, much of the excess current is envisioned to be carried by zinc cation vacancies, which are generated by ejection of cations from the cation sublattice of the barrier layer at the barrier layer/solution interface. If the zinc vacancies cannot be annihilated at the metal/barrier layer interface by the injection of cations from the metal via the reaction, $Zn + V_{Zn}^{2'} \rightarrow Zn_{Zn} + v_{Zn} + 2e^-$, the excess cation vacancies are envisioned to condense at the m/bl interface, thereby resulting in separation of the barrier layer from the substrate metal. Thus, vacancy condensation results in a cessation of growth of the barrier layer into the metal via $Zn \rightarrow Zn_{Zn} + V_O^{\bullet\bullet} + 2e^-$, but, of course, the barrier layer continues to dissolve at the bl/s interface as $ZnO + 2H^+ \rightarrow Zn_s^{2+} + H_2O$, where Zn_{Zn} and $V_O^{\bullet\bullet}$ are the zinc cation in a normal cation position in the barrier oxide layer and the oxygen vacancy on the anion sublattice in the same phase, respectively. Dissolution of the $Zn_{1+x}O_{1-y}$ at the bl/s interface that is unmatched by film growth at the m/bl interface eventually results in destruction of the passive film on the zinc and hence in activation of the galvanizing in its role as a sacrificial anode in protecting the adjacent steel in the scribe. This mechanism is essentially identical to that postulated by Macdonald, et. al. for passivity breakdown induced by aggressive anionic species, such as chloride ion, or film removal due to electro-polishing (4).

Summary and Conclusions

The work described in this paper was designed to establish the efficacy of the Module in reducing the development of corrosion damage on automobile panels and to indicate, to the extent possible, the mechanism by which protection is accomplished. The results of this study may be summarized as follows:

1. The Module is effective in protecting galvanized steel automotive body panels, as evidenced by a shift in the potential of the exposed steel at the scribe in the negative direction;

2. The mechanism of enhanced protection appears to be that the Module renders the zinc galvanizing (a sacrificial anode) more effective than when a Module is not connected to the system;

3. The mechanism of protection is not that of classical, impressed current cathodic protection. This is shown by the fact that the current or voltage applied to the panel by the Module is in the form of a repetitive pulse and not a direct current that is employed in impressed current cathodic protection systems, again demonstrating a vital difference between the latter and the Module. Furthermore, the system does not contain an anode or a continuous electrolyte path between the area of damage and any connection to the Module;

4. Unlike impressed current cathodic systems, the Module's effect is not limited to the region where a continuous electrolyte film exists between the point of application of the electrical current and the area being protected. Rather, similar to an antenna, the induced current from the Module covers the entire surface. As such, the Module is effective in reducing the rate of corrosion over the entire surface of a vehicle of complex shape. Furthermore, the frequency of the applied electrical signal is sufficiently high that the "skin effect", whereby current flow concentrates near the surface of a conductor, may become a factor in the mechanism of protection.

5. Activation of the zinc galvanizing by the electromagnetically-induced current occurs after an induction period. While the mechanistic details of the processes that determine the induction time are currently obscure, it is postulated that the generation of metal vacancies on the metal side of the m/bl interface result in vacancy condensation and separation of the barrier layer from the substrate metal, with the result that the barrier layer ceases to grow into the metal. However, the barrier layer continues to dissolve at the bl/s interface, with the result that the film thins and eventually ruptures, thereby activating the zinc as a sacrificial anode by exposing metallic zinc to the solution. In this manner, the Module is envisioned to enhance the efficacy of the galvanizing to protect the adjacent steel in the scribe.

Acknowledgments

The authors gratefully acknowledge the support of this work by Canadian Auto Preservation, Inc, Ontario, Canada.

References

1. S. M. Sharland, C. P. Jackson, and A. J. Dier, *Corros. Sci.*, **29**, 1149, (1989).
2. J. Young, "Measurement of Surface on a Typical Automobile Created by Canadian Auto Preservation Module", Report to Canadian Auto Preservation, Inc., by the Ohio State University Electrosciences Laboratory, Department of Electrical Engineering, Ohio State University, *Final Report 746284-1*, April 15, 2004.
3. Ismail, E. Sikora, and D. D. Macdonald, *J. Electrochem. Soc.*, **145**, 3141 (1998).
4. D. D. Macdonald, *Pure Appl. Chem.*, **71**, 951 (1999).